

## Exchange of simulation data between CFD programmes and a multi-segmented human thermal comfort model

Paul C Cropper<sup>1</sup>, Tong Yang<sup>1</sup>, Malcolm J Cook<sup>1</sup>, Dusan Fiala<sup>2</sup> and Rehan Yousaf<sup>1</sup>

<sup>1</sup>Institute of Energy and Sustainable Development, De Montfort University, Leicester LE1 9BH, UK

<sup>2</sup>Institute for Construction Economics, University of Stuttgart, Keplerstr. 11, 70174 Stuttgart, Germany

### Abstract

This paper describes the methods developed to extend the functionality of a commercial CFD program to provide a means of exchanging simulation data with a multi-segmented model of human thermal comfort and physiology.

A CFD model is able to predict detailed patterns and velocities of airflow around a human body, whilst a thermal comfort model is able to predict the response of a human to the environment surrounding it. By coupling the two models and exchanging information about the heat exchange at the body surface the coupled system can potentially predict the response of a human body to detailed local environmental conditions.

This paper presents a method of exchanging data between the two models using shared files. A test case is presented in which the results of a coupled system simulation are compared with experimental data of heat transfer coefficients predicted at the body surface under similar environmental conditions.

**Keywords:** CFD, Thermal Comfort, Heat Transfer Coefficient, Convection, Radiation, Computational Thermal Manikin

### Nomenclature

|          |                                      |                    |
|----------|--------------------------------------|--------------------|
| $T_0$    | Reference temperature                | °C                 |
| $T_{sf}$ | Surface temperature                  | °C                 |
| MRT      | Mean Radiant temperature             | °C                 |
| $Q_{sk}$ | Total heat flux at skin surface      | W/m <sup>2</sup>   |
| $Q_c$    | Convective heat flux                 | W/m <sup>2</sup>   |
| $Q_r$    | Long-wave radiative heat flux        | W/m <sup>2</sup>   |
| $Q_e$    | Evaporative heat flux                | W/m <sup>2</sup>   |
| $Q_{sR}$ | Short-wave heat flux                 | W/m <sup>2</sup>   |
| $h_c$    | Convective heat transfer coefficient | W/m <sup>2</sup> K |
| $h_r$    | Radiative heat transfer coefficient  | W/m <sup>2</sup> K |

## 1. Introduction

In an attempt to provide a comfortable environment for the occupants whilst at the same time reducing energy consumption, building designers are increasingly making use of natural ventilation as an alternative to air conditioning in non-domestic buildings. By its nature, natural ventilation is less tightly controlled when compared to air conditioning, and computer modelling is often used to predict the likely performance of a building design. Computational Fluid Dynamics (CFD) is a computer modelling technique that is able to predict in considerable detail complex patterns of airflow and air temperature distribution. It has been used successfully to predict the likely ventilation performance of many advanced naturally ventilated buildings (e.g. Cook and Short 2005, Short and Cook 2005). In design practice simple shaped blocks are often used to represent human occupants in CFD models and derive empirically-based thermal comfort parameters such as PMV and PPD.

A multi-segmented human thermal comfort model (the IESD-Fiala model) has been developed that can predict the response of the human body to varying environmental conditions and can predict the resulting degree of comfort or discomfort a person experiences (Fiala et al 2003). It has been extensively validated across a wide range of steady and transient indoor and outdoor environmental conditions. The IESD-Fiala model uses environmental parameters, such as the temperature, humidity and velocity of air at the skin surface, to predict the response of the human thermoregulatory system to these external stimuli over a period of time.

The aim of the research project described is to use a commercial CFD model to predict the local environmental conditions around a human body in a naturally ventilated building and to use the IESD-Fiala model to predict the response of a human body to those conditions, both the degree of comfort or discomfort experienced and temperature changes at the body surface. Changes in temperature at the body surface are fed back to the CFD model to enable the effect that the body has on the local environment to be taken into account. This two-way data transfer is thought to be particularly important when modelling naturally ventilated spaces where air velocities are low, due to the small driving forces. In such cases, the effect that a human body has on the local environment is potentially more significant than in other environments where velocities are higher.

Various degrees of coupling systems have been reported. For example Murakami et al. (2000) and Al-Mogbel (2003) used a simplified shape to represent a human body in CFD and coupled this with a two-node thermal regulatory model (Gagge et al 1986). Tanabe et al. (2002) integrated a 65-node human thermoregulatory model with a 3D model of a nude male body in CFD which incorporated radiation heat transfer. Similarly, Omori et al. (2004) coupled a realistic nude female body with a PMV model (Fanger, 1970). This research considers more realistic, clothed bodies in representative typical indoor environments. The research project uses CFD techniques to predict local environmental parameters for 59 regions of the human body, to dynamically exchange those parameters with the IESD-Fiala model to enable human thermal comfort to be predicted along with the effect the body has on its surroundings and to enable building designers to directly assess the impact of design decisions on occupant comfort. Consequently, a better understanding and innovative control strategies of indoor environments could be developed. As a result, providing effective design tools to improve building thermal performance and occupant comfort and reduce energy consumption.

This paper describes a new coupled system of integrating CFD with the IESD-Fiala model. The system is designed using user subroutines to interact with the CFD solver. The intention is that the techniques developed will be applicable to any CFD platform which offers user-

accessible development tools. The coupled system is demonstrated by application to a person standing in a naturally ventilated test environment. The success of the coupled system is assessed by comparing predicted heat transfer coefficients with experimental data obtained under similar test conditions.

## 2. Multi-segmented thermal comfort model

The IESD-Fiala thermal comfort model consists of two interacting systems: the controlling active system; and the controlled passive system. The active system (Fiala et al 2001) is a cybernetic model predicting the thermoregulatory defence reactions of the central nervous system. The passive system (Fiala et al 1999) simulates the physical human body and the dynamic heat transfer phenomena that occur inside the body and at its surface.

The IESD-Fiala model also incorporates a physiologically based thermal comfort model (Fiala et al 2003) which predicts human thermal sensation responses in steady state and transient conditions.

### 2.1 Active system

A human being maintains internal temperature at a fairly constant value using four essential thermoregulatory responses; vasoconstriction, vasodilatation, shivering and sweating. Peripheral vasomotion, via suppression (vasoconstriction) and elevation (vasodilatation) of the skin blood flow, is activated to regulate internal temperature in moderate environments. In cold conditions, vasoconstriction is accompanied by shivering, i.e. a regulatory increase in the metabolic heat generation by contraction of muscle fibres. In warm and hot conditions, vasodilatation is accompanied by sweating, i.e. excretion of moisture at the skin which evaporates cooling the body.

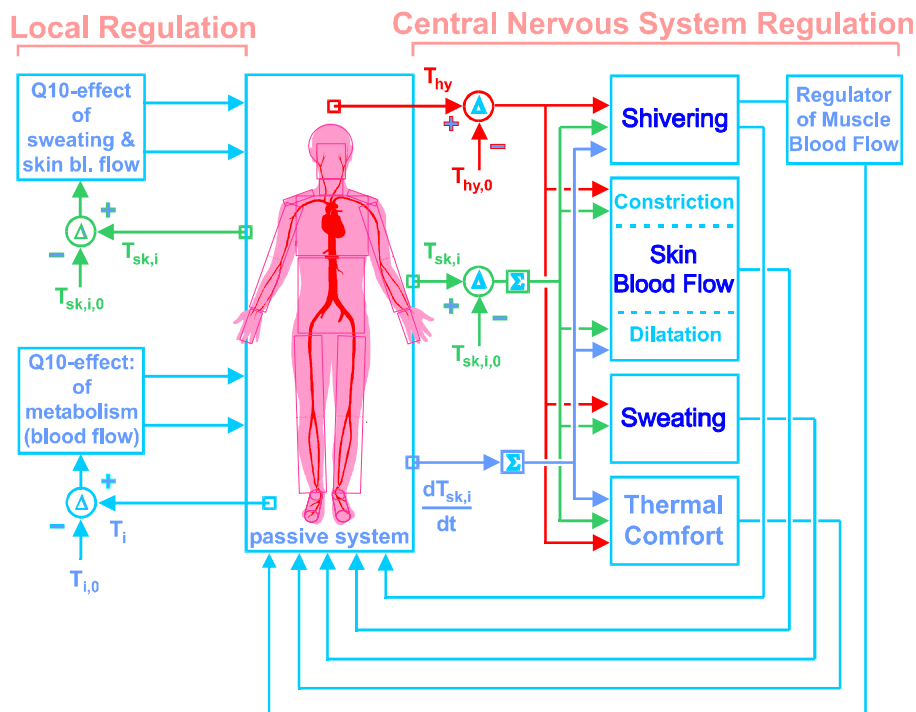


Figure 1 Block diagram of the active system of the IESD-Fiala model

The active system was developed by means of statistical regression using measured data obtained from numerous physiological experiments covering steady state and transient cold stress, cold, moderate, warm and hot stress conditions, and activity levels of up to heavy exercise. A block diagram of the active system model is shown in

*Figure 1.*

## 2.2 Passive System

The passive system is a multi-segmental, multi-layered representation of the human body with spatial subdivisions and detailed information about anatomic and geometrical body properties. The body is idealised as 19 spherical and cylindrical elements built of annular concentric tissue layers with the appropriate thermo-physical properties and physiological functions. Tissue layers are subdivided further into spatial sectors and discretised into a total of 317 tissue nodes (Figure 2). The division of these elements into sectors yields a total of 59 areas at the body surface. The standard model represents an average person with a body weight of 73.5 kg, body fat content of 14%wt, Dubois-area of 1.86 m<sup>2</sup>, basal metabolism of 87 W, basal evaporation from the skin of 18W, and basal cardiac output of 4.9 L/min. The sizes and composition of the 19 body elements, including the thickness and characteristics of each of the tissue layers, are contained in a data file, enabling different body characteristics to be modelled. Similarly, the regions of the body covered by clothing and the thermal characteristics of that clothing are also contained in a data file, enabling different levels of clothing to be modelled.

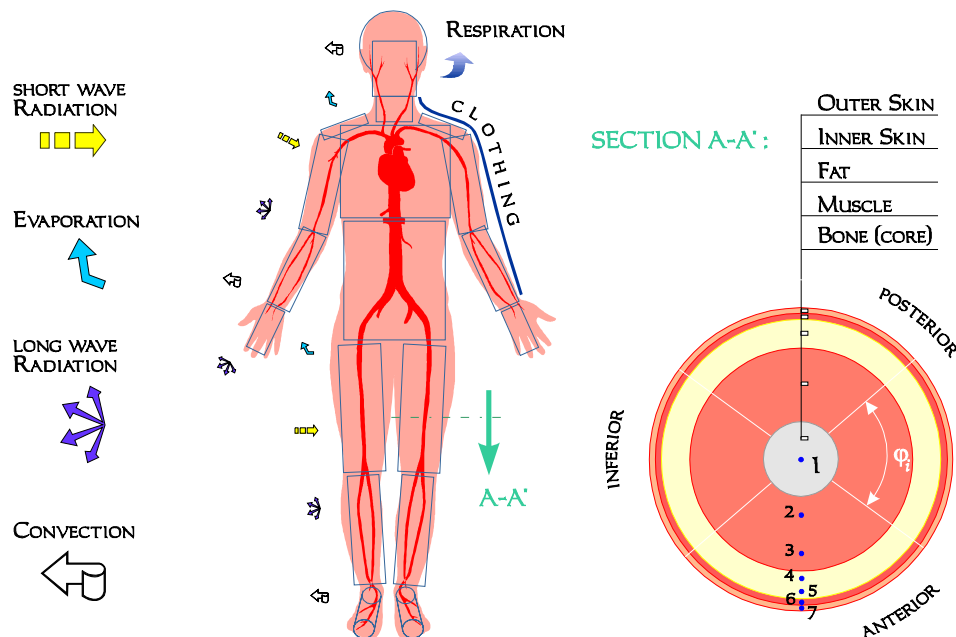


*Figure 2 A schematic diagram of the passive system model*

Within the human body, metabolic heat is produced which is distributed over body regions by blood circulation and heat conduction from warmer to colder tissue locations.

For each sector of the passive system heat balances are established as boundary conditions at the surface. The net skin heat loss,  $Q_{sk}$  [W/m<sup>2</sup>] of a sector exposed to ambient air is equivalent to the sum of individual components of the environmental heat loss (equation 1).

$$Q_{sk} = Q_c + Q_r + Q_e + Q_{sR} \quad (1)$$

where  $Q_c$  [ $\text{W}/\text{m}^2$ ] is the heat exchange by free and forced convection with ambient air,  $Q_r$  [ $\text{W}/\text{m}^2$ ] the long-wave thermal radiation exchange with surrounding surfaces,  $Q_e$  [ $\text{W}/\text{m}^2$ ] the latent heat loss from the skin due to moisture diffusion and sweat liquid evaporation and  $Q_{sR}$  [ $\text{W}/\text{m}^2$ ] the absorption of direct and diffuse solar (short-wave) irradiation.

### 2.3 Environmental conditions

The IESD-Fiala model predicts the response of the human body to the environmental conditions surrounding the body, such as the air temperature, air speed (velocity) and the radiative heat exchange with surrounding surfaces. In this research a CFD model is used to predict the convective heat flux  $Q_c$  and long-wave radiative heat flux  $Q_r$  at the skin surface of the 59 body parts. During this ongoing research the data exchange will be extended to include the parameters required to calculate the evaporative heat flux  $Q_e$  resulting from the evaporation of moisture on the skin surface (sweating) and the effect of short-wave irradiation.

### 2.4 Revised body geometry

In this research, the idealised body geometry described above is replaced by a more realistic three-dimensional representation of a clothed human body, termed a computational thermal manikin (CTM) (Yang et al 2007), with a surface area of  $2.019\text{m}^2$ . The manikin, illustrated in Figure 3, represents a casually dressed typical male with a height of  $1.73\text{m}$ . The manikin geometry has been optimised, particularly in areas such as the hands, the underarms and the crotch, to allow a CFD mesh to be constructed around it.

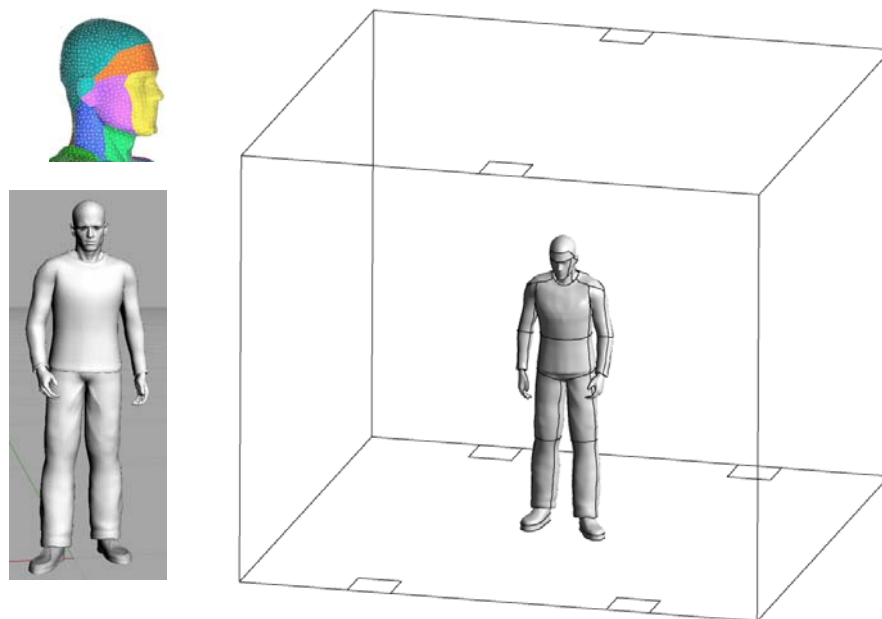


**Figure 3** A clothed computational thermal manikin in a naturally ventilated room with upper and lower openings.

## 3. CFD Modelling

The commercial CFD code ANSYS CFX (ANSYS, 2007), version 11, was used to model air flow and heat transfer in this work. Steady-state simulations have been used to model the thermal conditions in an indoor environment with a human body as the only heat source. The

software employs a coupled, fully implicit solver using a transient evolution of the flow from the initial conditions. The physical timesteps used in the transient evolution provide a means of controlling the solution procedure. CFX uses a multi-element type mesh comprising hexahedrals, tetrahedrals, wedges and pyramids. The conservation equations are solved using the Finite Volume method (Versteeg and Malalasekera 1995). Flow variables (velocity, pressure, enthalpy, etc) are defined at the corners of each element which are located at the centre of each control volume used for solving the conservation equations.

#### **4. Model Coupling**

In the coupled simulation, the IESD-Fiala model predicts temperatures at the body surface in response to the environmental conditions surrounding the body. The CFD model predicts the environmental conditions surrounding the body, including the effect the warm body has on that environment. The CFD model also predicts the heat transfer (heat flux) at the body surface resulting from differences between the body surface temperature, the air temperature, the air movement (velocity) and the temperature of surrounding surfaces. The predictions produced by each computer model effect the predictions produced by the other. The coupled simulation is therefore an iterative process in which the two models attempt to arrive at a consensus.

##### **4.1 Data exchange**

Two method of exchanging data between the models were considered; network sockets and data files. A network socket, identified by a unique (socket) number, provides a dedicated channel of communication between two computers connected via a computer network. The use of network sockets is an appropriate technique when two computer models are to be run on different computer systems. This method has previously been successfully used to couple the IESD-Fiala model with the INKA car simulator (Fiala et al 2004). In this research the two computer models run on the same computer system. A simple approach using locally stored files is therefore employed.

Two types of file are used in the data exchange process; files containing data and empty files used to control the data transfer process. To transfer data to the CFD model, the IESD-Fiala model creates a data file containing a list of body parts and their surface temperatures. When the IESD-Fiala model has finished writing to the data file it creates a second (empty) file to indicate to the CFD model that new surface temperature data are available. To transfer data to the IESD-Fiala model, the CFD model creates a data file containing the mean air temperature, the mean radiant temperature and a list of body parts and their corresponding convective and radiative heat flux values. When the CFX model has finished writing to the data file it creates a second (empty) file to indicate to the IESD-Fiala model that new temperature and flux data are available.

##### **4.2 CFD solver customisation**

The chosen commercial CFD solver, ANSYS CFX, provides facilities to enable users to extend the functionality of the solver by writing additional computer code.

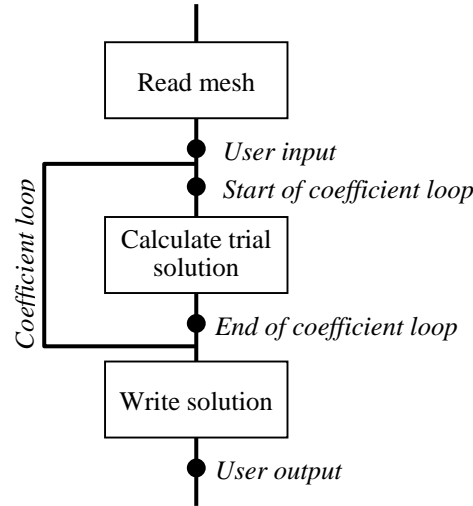


**Figure 4** CFD simulation cycle

This additional code, written in FORTRAN, can be subroutines that are executed at specific stages of the simulation cycle, to control the solver or to perform tasks such as reading and writing files, or functions to provide numeric values to the solver calculations. Some of the specific stages in the CFD simulation cycle where user written subroutines can be executed are illustrated in Figure 4.

### 4.3 The coupled simulation cycle

At the *User input* stage in the CFD simulation cycle, a user written subroutine loads initial surface temperatures provided by the IESD-Fiala model into the CFD model. A user written function is then used to supply these values to the solver calculations in place of the usual predefined fixed values.

At the *End of coefficient loop* stage in the CFD simulation cycle, a user written subroutine determines if the CFD model has reached a sufficient degree of convergence (see section 4.4) for data exchange between the two models to take place. If the convergence criteria are met, a data file is generated containing the volume averaged room temperature, the mean radiant temperature and the convective heat flux and the radiative heat flux for each of the 59 body parts. Once writing to the data file has been completed, an empty file is produced, the existence of which indicates to the IESD-Fiala model that data is available from the CFD model. The CFD model then waits for the IESD-Fiala model. If the convergence criteria are not met the CFD simulation cycle continues using the same surface temperature values.

The IESD-Fiala model uses the data supplied to calculate a convective and a radiative heat transfer coefficients for each body part by transposing the following equations.

$$Q_c = hc(T_{sf} - T_0) \quad (2)$$

$$Q_r = hr(T_{sf} - MRT) \quad (3)$$

where  $Q_c$  is the convective heat flux,  $hc$  is the convective heat transfer coefficient,  $Q_r$ , is the radiative heat flux,  $hr$  is the convective heat transfer coefficient,  $T_{sf}$  is the surface temperature,  $T_0$  is the reference air temperature and  $MRT$  is the mean radiant temperature. These are used by the IESD-Fiala model to predict new surface temperatures, which are written to a data file. Once writing to the data file has been completed, an empty file is produced, the existence of which indicates to the CFD model that new surface temperatures are available. These are then loaded into the CFD model and the CFD simulation resumed.

This process is repeated until the coupled system achieved overall convergence (see section 4.4).

#### **4.4 Coupled system convergence**

The IESD-Fiala model is a dynamic model that predicts how the human body responds over time to changing environmental conditions. However, the coupled simulation technique described in this paper models steady state conditions. The IESD-Fiala model is therefore run in a way that simulates exposing the body to these steady state conditions for a period of time, by running the model with incrementing time steps whilst keeping the environmental conditions the same until the mean body surface temperature changes by less than 0.001 °C between iterations. The IESD-Fiala model therefore achieves internal convergence each time it runs.

A CFD simulation is deemed to have achieved convergence when the residual values at the end of an iteration fall below a level specified by the user, usually  $10^{-4}$  or  $10^{-5}$ . In the coupled simulation the two models begin exchanging data once the CFD residual values have fallen below  $10^{-3}$ . After a few CFD model iterations, data is exchanged again provided that the residual values remain below  $10^{-3}$ . The two models continue to exchange data until the CFD model achieves the level of convergence required by the user. Overall convergence of the coupled system is therefore achieved at this point and the simulation terminated (because the IESD-Fiala model has already achieved convergence).

### **5. Details of test case**

#### **5.1 Environmental conditions**

For the test case described in this paper, the manikin is modelled in the centre of a naturally ventilated room  $3\text{m} \times 3\text{m} \times 2.5\text{m}$  (length  $\times$  width  $\times$  height) as shown in Figure 3. The room has four floor level openings, each  $0.25\text{m} \times 0.25\text{m}$ , adjacent to the front and rear walls and 0.75m from the side walls. A further two openings of the same size are located in the ceiling adjacent to the front and back walls in the centre of the room. The initial air temperature in the room is set to 20°C with a relative humidity of 50%. The wall temperatures are modelled with a fixed temperature of 20°C. All openings are given a pressure boundary setting of 0 Pa and air is free to flow in either direction depending on the local pressure differences resulting from buoyancy forces. The conduction heat exchange between shoes and floor is considered to be negligible compared to total heat loss of the body and is therefore not considered in the current study.

#### **5.2 The CFD model**

The manikin, which is subdivided into 59 body parts, has a total of 66,611 surface mesh elements. Turbulence is modelled using the Shear Stress Transport (SST) turbulence model which was chosen for its ability to resolve flow field variables within the boundary layer around the human body (Menter 1994). There are 10 prism layers are placed near manikin body and walls (see Figure 5). The computational domain is composed of approximately 1.6 million unstructured and structured elements.

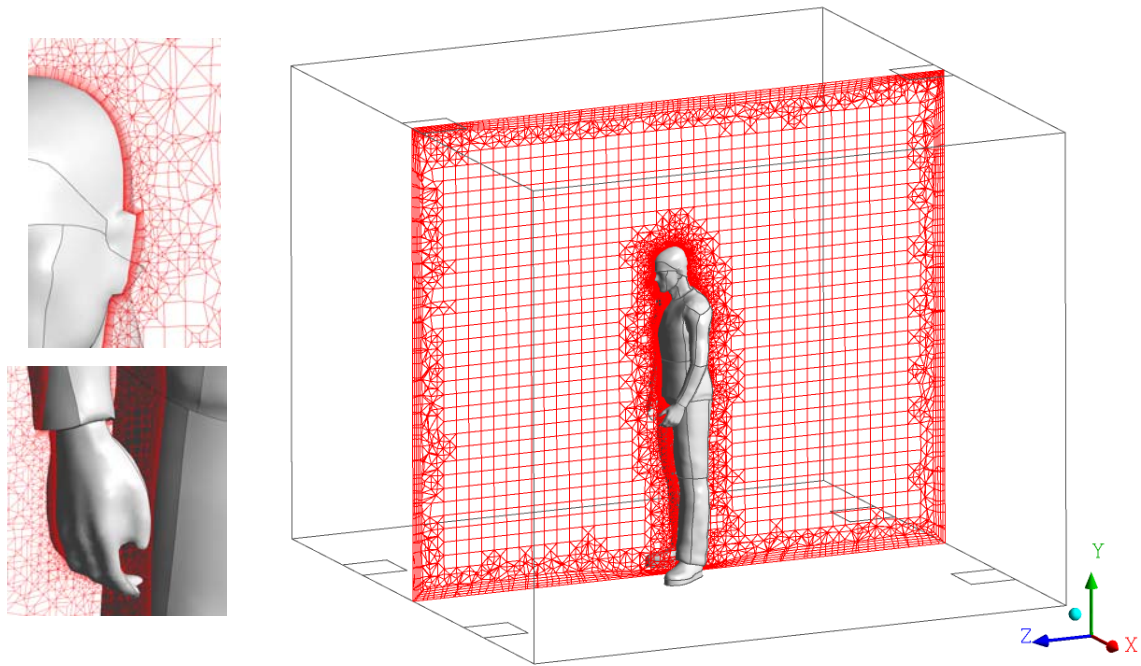


**Figure 5** A section view of CFD mesh

As the indoor temperature differences are relatively small, the Boussinesq approximation is used to model the effects of buoyancy. Initial tests and previous studies by Zitzmann et al. (2007) showed that modelling radiation between a detailed human model and its surroundings in a simple room using the Monte Carlo method with 2 million tracking histories gave unrealistic temperature distributions on the body surfaces. To avoid this, the Discrete Transfer model was used with 16 rays. This also led to a saving of 98% in computing time. Emissivity for all surfaces is assumed to be uniform at 0.95.

### 5.3 Model comparison

The convective and radiative heat transfer coefficients predicted by the coupled system are compared with experimental data of de Dear et al. (1997). Although the CTM body geometry used in the coupled system represents a clothed figure, for this comparison zero clothing insulation (0 clo) was specified.

For the coupled system simulation, the surface temperatures of the 59 body regions were determined by the IESD-Fiala model and updated during the coupled simulation in response to the environmental conditions predicted by the CFD model.

The convective and radiative heat transfer coefficients predicted by the coupled system were compared with the empirical coefficients obtained by de Dear et al (1997) in which a nude female manikin, whose skin temperature was maintained at a constant temperature, was placed in a test chamber. In this experiment, heat transfer coefficients were determined by measuring the energy required to maintain a constant surface temperature over 16 body regions, i.e. the energy required to replace the heat lost to the local environment. The combined heat loss, i.e. the sum of the convective and radiative components, was first determined. Selected areas of the manikin were then covered by a low Emissivity material and the experiment repeated in order to isolate the radiative component.

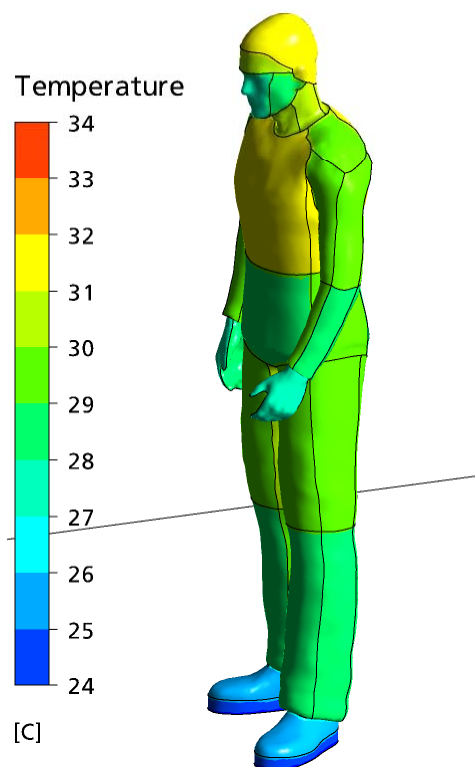
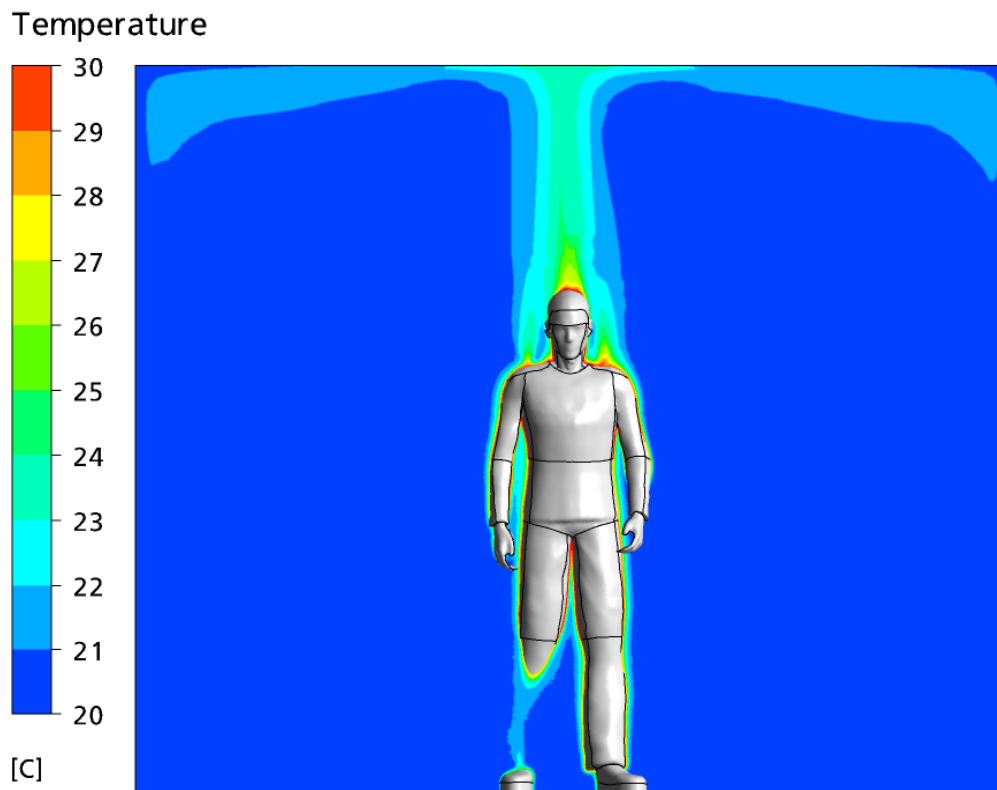


*Figure 5 Air temperature distribution over the central cross section and surface temperature distribution over the CTM*

## 6. Results

The coupled simulation for the test case described in this paper was run on a multi-processor Linux computer cluster, consisting of multiple 3.83 GHz Intel Xeon quad-core processors with 8GB of RAM per processor (2GB per core). The simulation took approx. 1.75 hours to run using 16 processor cores. The simulation results are obtained using a second-order discretization scheme. The normalised root-mean-square (RMS) residuals of all equations reached  $5 \times 10^{-5}$ . The maximum value of  $y^+$  (the dimensionless distance between the wall and first node) for each body part is 1.1 with an average value of 0.7.

The spatial air temperature distribution and surface temperature on the computational thermal manikin (CTM) body parts are shown in Figure 6. It can be seen that the coupled system predicts a non-uniform surface temperature in this test environment with the head and upper torso predicted to be at a higher temperature than the hands, legs and feet.

It can be seen in Figure 7 that the thermal plume develops over the height of the body and reaches a maximum speed of about 0.35m/s at about 0.5m above the head.

The predicted convective heat transfer coefficients are compared with the experimental results (de Dear et al 1997) in Figure 8 and the predicted radiative heat transfer coefficients are compared with the experimental results in Figure 9.

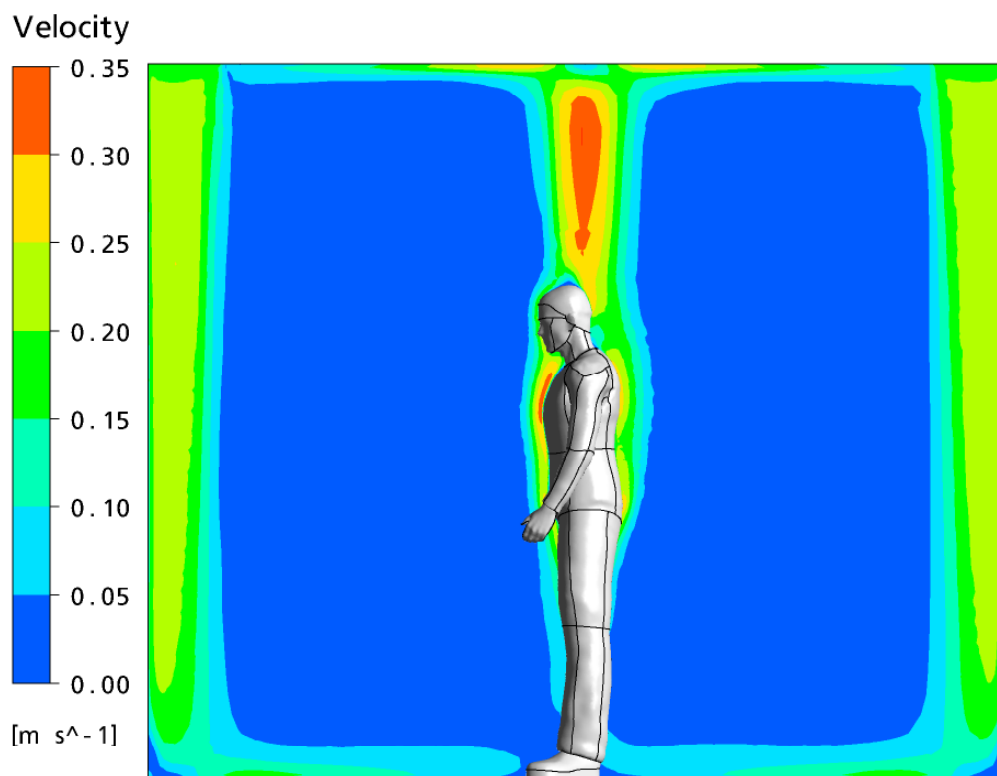
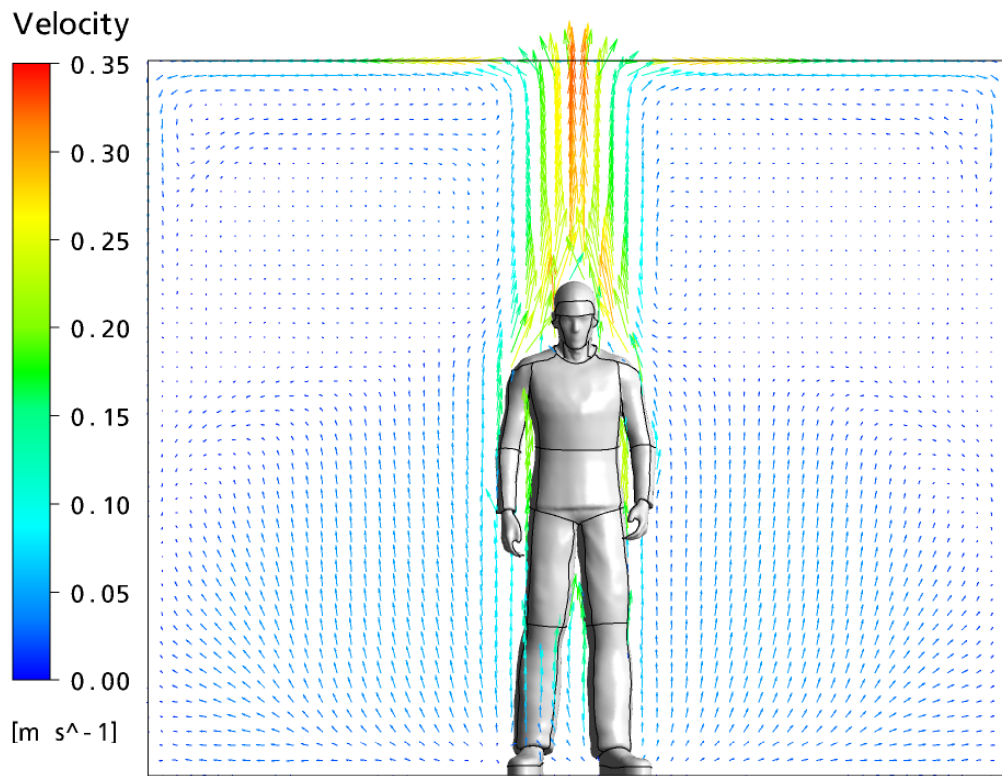


*Figure 5 Air speed distributions over the central cross sections*

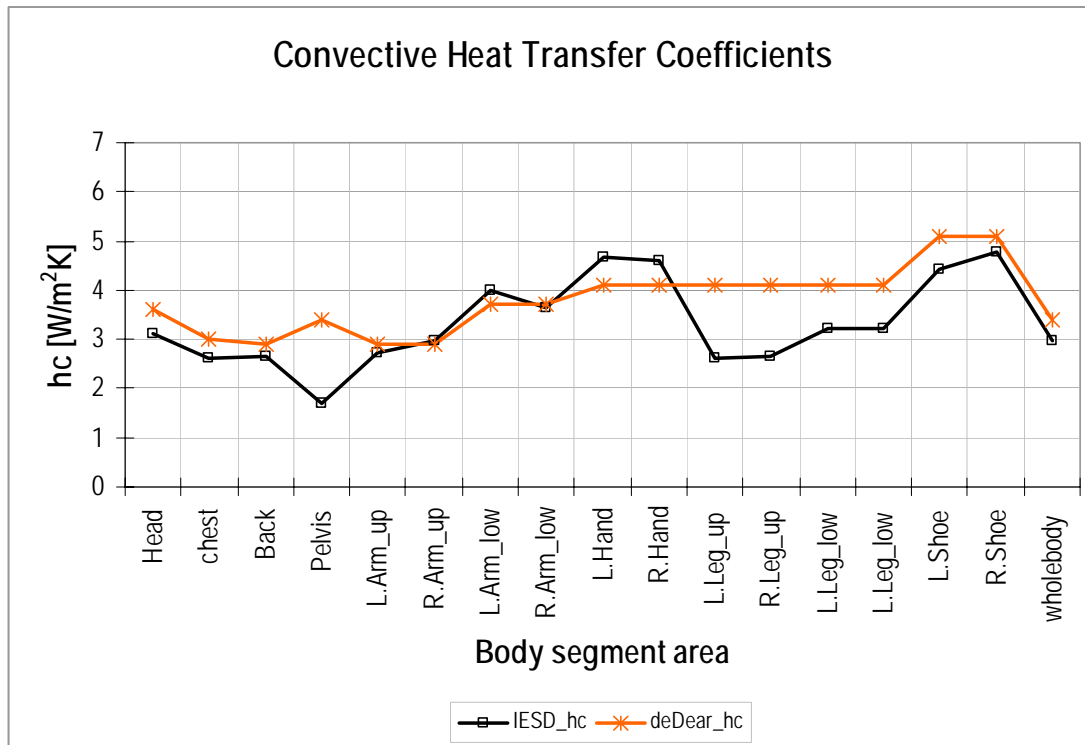


**Figure 6 Comparison of convective heat transfer coefficients**

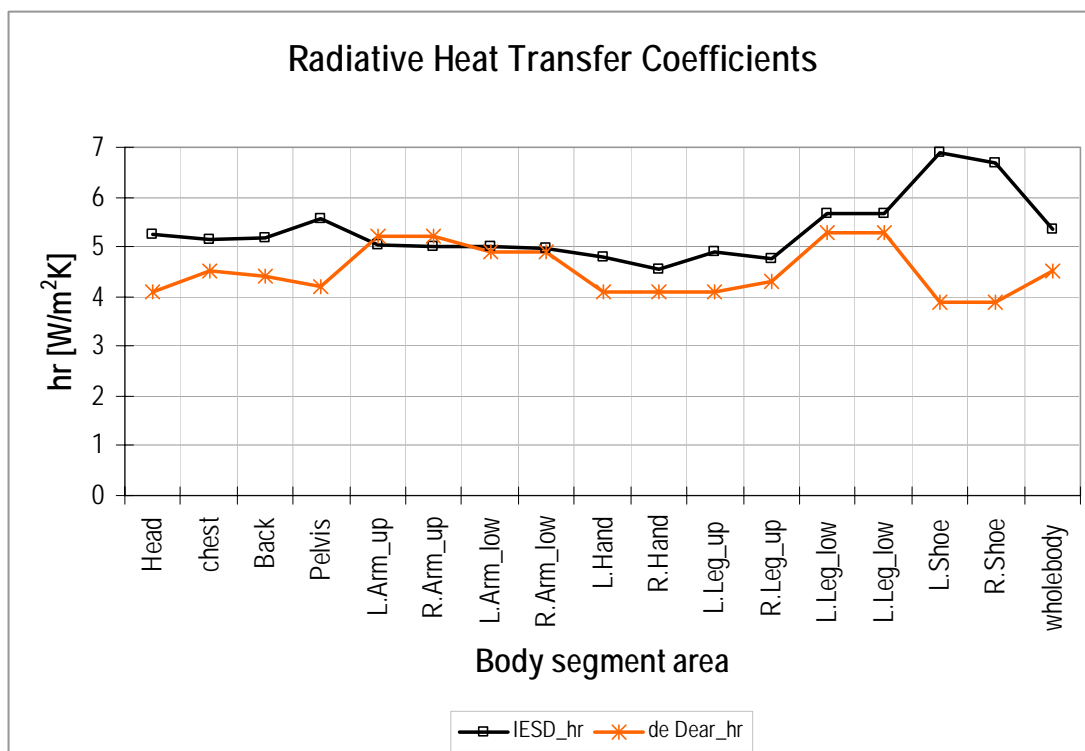


**Figure 7 Comparison of radiative heat transfer coefficients**

It can be seen that although the agreement between the predicted and experimental results is encouraging there are significant differences in some areas of the body. The reasons for these differences are still under investigation but they are thought to include some or all of the following:

- In the coupled simulations, the body surface temperatures were determined by the IESD-Fiala model whilst in the de Dear experiments the body surface temperatures were held at a constant value relative to the surrounding air temperature. It is likely that these different methods of calculating heat transfer coefficients will result in differences in the distribution of heat transfer over the body surfaces.
- Although modelled as a nude figure, i.e. without the insulating effect of clothing, the CTM body geometry used in the coupled simulations corresponds to a clothed figure, resulting in differences in surface areas.
- The CTM is divided into 59 regions whilst the experimental manikin is divided into 16 regions. It was therefore necessary to combine heat transfer coefficient values from several CTM regions when comparing predictions with experimental results. It was not possible to match the regions exactly due to differing region boundaries.
- Differences in the overall body shape, body posture and at the body surface caused by the presence of clothing may have an impact on the development of air flow patterns around the body and the radiative heat exchange.

The convective and radiative heat transfer coefficients predicted by the coupled system for 59 body parts are given in Table A1 in Appendix A.

## **7. Conclusions**

A new coupled simulation technique has been developed that enables a multi-segmented model of human thermal comfort and physiology to exchange data with a commercial CFD program.

Comparisons of the predictions by the coupled system with published experimental data show favourable agreement on the overall whole body mean heat transfer coefficients in still air conditions. The differences which occur in some body parts are thought to be due, in part, to the differences in surface area between the CTM and the experimental nude female manikin and posture. There are however, noticeable differences in some regions of the body which require further investigation.

In the coupled simulation system described in this paper, only convective and radiative heat fluxes are exchanged. The coupling technique will be extended to include heat loss due to evaporation (sweating) and heat gain due to short-wave radiation.

The comparisons described in the paper represent a relatively simple case, in which the manikin is placed in an initially uniform environment. Future studies will investigate the responses of the coupled system to more challenging and non-uniform environments.

## **Acknowledgements**

The authors wish to acknowledge the Engineering and Physical Sciences Research Council (EPSRC) for their support for this research through grant ref. EP/C517520/1.

The authors wish to gratefully acknowledge the technical support provided by Chris Staples, CFX Technical Services, ANSYS Europe Ltd.

## References

- Al-Mogbel A, (2003), *A coupled model for predicting heat and mass transfer from a human body to its surroundings*, Proc. 36<sup>th</sup> AIAA Thermophysics Conference Florida, AIAA 2003-4211.
- ANSYS Inc, (2007), ANSYS CFX Help, Release 11.0, *ANSYS CFX Users Guide*, <http://www.ansys.com>
- Cook MJ and Short CA, (2005), *Natural Ventilation and Low Energy Cooling of Large, Non-Domestic Buildings - Four Case Studies*, The International Journal of Ventilation, Vol. 3 No 4, pp 283-294.
- de Dear, RJ, Arens A, Hui Z and Oguro M, (1997), *Convective and radiative heat transfer coefficients for individual body segments*, International Journal of Biometeorology, Vol. 40, pp 141-156.
- Fanger, PO, (1970), *Thermal comfort*. Danish Technical Press, Copenhagen, Denmark.
- Fiala D, Lomas KJ and Stohrer M, (1999), *A computer model of human thermoregulation for a wide range of environmental conditions: The passive system*, Journal of Applied Physiology, Vol. 87 (5), pp 1957-1972.
- Fiala D, Lomas KJ and Stohrer M, (2001), *Computer prediction of human thermoregulatory and temperature responses to a wide range of environmental conditions*, International Journal of Biometeorology, Vol. 45, pp 143-159.
- Fiala D, Lomas, KJ and Stohrer M, (2003), *First Principles Modelling of Thermal Sensation Responses in Steady State and Transient Boundary Conditions*, ASHRAE Transactions, Vol. 109 (1), pp179-186.
- Fiala D, Bunzl A, Lomas KJ, Cropper PC and Schlenz D, (2004), *A new simulation system for predicting human thermal and perceptual responses in vehicles*, in Schlenz D (Ed) PKW-Klimatisierung III: Klimakonzepte, Regelungsstrategien und Entwicklungsmethoden, Haus der Technik Fachbuch, Expert Verlag, Renningen, Band 27, pp 147-162, ISBN 3 8169 2268 6.
- Gagge A, Fobelets A, and Berglund L, (1986), *A standard predictive index of human response to the thermal environment*, ASHRAE Trans 92(2): 709-731.
- Menter FR, (1994), *Two-equation eddy-viscosity turbulence models for engineering applications*, AIAA Journal 32, pp 1598-1605.
- Murakami S, Kato S and Zeng J, (2000), *Combined simulation of airflow, radiation and moisture transport for heat release from a human body*, Building and Environment, 35(6): 489-500.
- Omori T, Yang JH, Kato S and Murakami S, (2004), *Coupled Simulation of Convection and Radiation on Thermal Environment around an Accurately Shaped Human Body*. Proc. 9<sup>th</sup> international conference - RoomVent 2004. Portugal, pp.7.
- Short CA and Cook MJ, (2005), *Design Guidance for Naturally Ventilated Theatres*, Building Services Engineering Research and Technology, Vol. 26, No. 3, pp 259-270.
- Tanabe S, Kobayashi K, Nakano J, Ozeki Y and Konishi M, (2002), *Evaluation of thermal comfort using combined multi-node thermoregulation (65MN) and radiation models and computational fluid dynamics (CFD)*, Energy and Buildings, 34(6): 637-646.
- Versteeg HK and Malalasekera W, (1995). *An introduction to computational fluid dynamics – the finite volume method*, Longman Group Ltd. ISBN 0-582-21884-5.
- Yang T, Cropper PC, Cook MJ, Yousaf R and Fiala D, (2007), *A new simulation system to predict human-environment thermal interactions in naturally ventilated buildings*, Proc. 10<sup>th</sup> International Building Performance Simulation Association Conference and Exhibition (BS2007), Beijing, China, pp751-756.
- Zitzmann T, Cook M and Pfrommer P, (2007), *Dynamic CFD modelling of thermal mass and air movement*, International Journal of Ventilation, 6(2): 145-156.

## Appendix A

The convective and radiative heat transfer coefficients predicted for the 59 regions of the CTM are given in Table A1 below.

**Table A1, Predicted convective and radiative heat transfer coefficients for 59 body parts of the computational thermal manikin**

| no. | Body part name | hc<br>[W/m <sup>2</sup> K] | hr<br>[W/m <sup>2</sup> K] | No. | Body part name | hc<br>[W/m <sup>2</sup> K] | hr<br>[W/m <sup>2</sup> K] |
|-----|----------------|----------------------------|----------------------------|-----|----------------|----------------------------|----------------------------|
| 1   | Forehead       | 5.40                       | 5.67                       | 32  | R.Arm_low_ant  | 2.52                       | 5.24                       |
| 2   | Head           | 2.74                       | 5.40                       | 33  | R.Arm_low_ext  | 3.33                       | 6.34                       |
| 3   | Face_ant       | 4.82                       | 6.25                       | 34  | R.Arm_low_inf  | 4.24                       | 2.33                       |
| 4   | Face_ext_L     | 2.60                       | 5.53                       | 35  | R.Arm_low_pst  | 4.35                       | 5.99                       |
| 5   | Face_ext_R     | 2.61                       | 5.37                       | 36  | L.Hand_back    | 4.80                       | 6.28                       |
| 6   | Neck_ant       | 3.65                       | 3.68                       | 37  | L.Hand_palm    | 4.47                       | 2.76                       |
| 7   | Neck_ext_L     | 2.41                       | 4.52                       | 38  | R.Hand_back    | 4.98                       | 6.42                       |
| 8   | Neck_ext_R     | 2.52                       | 4.32                       | 39  | R.Hand_palm    | 4.08                       | 2.25                       |
| 9   | Neck_pst       | 1.24                       | 4.96                       | 40  | L.Leg_up_ant   | 2.42                       | 5.60                       |
| 10  | L.Shoulder     | 1.39                       | 5.57                       | 41  | L.Leg_up_ext   | 2.49                       | 5.88                       |
| 11  | R.Shoulder     | 1.34                       | 5.57                       | 42  | L.Leg_up_inf   | 2.79                       | 2.23                       |
| 12  | Thorax_ant     | 2.72                       | 5.37                       | 43  | L.Leg_up_pst   | 2.85                       | 5.67                       |
| 13  | Thorax_inf_L   | 3.26                       | 3.55                       | 44  | R.Leg_up_ant   | 2.67                       | 5.66                       |
| 14  | Thorax_inf_R   | 3.52                       | 3.54                       | 45  | R.Leg_up_ext   | 2.50                       | 5.11                       |
| 15  | Thorax_pst     | 2.71                       | 5.52                       | 46  | R.Leg_up_inf   | 2.77                       | 2.46                       |
| 16  | Abdomen_ant    | 1.43                       | 5.78                       | 47  | R.Leg_up_pst   | 2.57                       | 5.96                       |
| 17  | Abdomen_inf_L  | 1.95                       | 4.89                       | 48  | L.Leg_low_ant  | 2.85                       | 6.14                       |
| 18  | Abdomen_inf_R  | 1.84                       | 4.22                       | 49  | L.Leg_low_ext  | 3.08                       | 6.29                       |
| 19  | Abdomen_pst    | 1.75                       | 6.33                       | 50  | L.Leg_low_inf  | 3.09                       | 4.26                       |
| 20  | L.Arm_up_ant   | 2.30                       | 5.24                       | 51  | L.Leg_low_pst  | 3.90                       | 6.05                       |
| 21  | L.Arm_up_ext   | 2.71                       | 6.14                       | 52  | R.Leg_low_ant  | 3.23                       | 5.81                       |
| 22  | L.Arm_up_inf   | 4.57                       | 1.21                       | 53  | R.Leg_low_ext  | 2.69                       | 6.24                       |
| 23  | L.Arm_up_pst   | 2.24                       | 5.60                       | 54  | R.Leg_low_inf  | 3.15                       | 4.37                       |
| 24  | R.Arm_up_ant   | 2.37                       | 5.34                       | 55  | R.Leg_low_pst  | 3.55                       | 6.38                       |
| 25  | R.Arm_up_ext   | 2.53                       | 6.11                       | 56  | L.Shoe_upper   | 2.98                       | 7.58                       |
| 26  | R.Arm_up_inf   | 4.79                       | 1.20                       | 57  | L.Shoe_low     | 7.11                       | 6.91                       |
| 27  | R.Arm_up_pst   | 2.96                       | 5.79                       | 58  | R.Shoe_upper   | 3.01                       | 6.74                       |
| 28  | L.Arm_low_ant  | 2.64                       | 5.30                       | 59  | R.Shoe_low     | 7.39                       | 6.67                       |
| 29  | L.Arm_low_ext  | 3.79                       | 6.48                       |     |                |                            |                            |
| 30  | L.Arm_low_inf  | 5.15                       | 2.55                       |     | Whole body     | 2.97                       | 5.47                       |
| 31  | L.Arm_low_pst  | 4.47                       | 5.82                       |     |                |                            |                            |